PHYSICAL REVIEW D **87,** 114506 (2013)

# Formulation of domain-wall fermions in the Schrödinger functional

Shinji Takeda*

*Physics Department, Columbia University, New York, New York 10027, USA*

(Received 16 May 2013; published 11 June 2013)

We present a formulation of domain-wall fermions in the Schrödinger functional by following a universality argument. To examine the formulation, we numerically investigate the spectrum of the free operator and perform a one-loop analysis to confirm universality and renormalizability. We also study the breaking of the Ginsparg-Wilson relation to understand the structure of chiral symmetry breaking from two sources: the bulk and the boundary. Furthermore, we discuss the lattice artifacts of the step scaling function by comparing with other fermion discretizations.

DOI: 10.1103/PhysRevD.87.114506 PACS numbers: 11.15.Ha

## I. INTRODUCTION

In the study of $CP$ violation by CKM unitary triangle analysis, hadron matrix elements of four-fermion operators, such as $B_{\mathrm{K}}$, play a vital role. Accurate calculations of this quantity from first principles are important for the lattice QCD community. In such calculations, having chiral symmetry is crucial to avoid an operator mixing problem that requires extremely high accuracy. Although lattice chiral fermions [1–3] are a clean formulation, they require enormous computing power to perform dynamical simulations. In comparison, ordinary fermion formulations, like Wilson-type fermions and staggered fermions, are relatively cheap. Nowadays, however, thanks to the development of computer architecture and algorithms, dynamical simulations with lattice chiral fermions have become feasible even for three flavors [4]. In particular, the RBC/UKQCD Collaboration [5] is currently using domain-wall fermions (DWFs) to compute $B_{\mathrm{K}}$. In the course of their computation, there are many sources of systematic errors that one has to control. Among them, the nonperturbative renormalization could be serious. At the moment, the collaboration has been using conventional schemes, such as the RI/MOM scheme and its variants [6,7]. However, these schemes potentially contain a ''window problem,'' which requires a quite large lattice volume. To avoid such difficulties, a new scheme was invented, known as the Schrödinger functional (SF) scheme [8]. This scheme provides a reliable way of estimating errors in the nonperturbative renormalization. If one wants to use this scheme for the renormalization of $B_K$ given by the RBC Collaboration, first of all, one has to formulate DWF in the SF setup. This is the purpose of the present paper.

While chiral fermions are useful for computing the bare $B_{\mathrm{K}}$ to avoid the mixing problem, a formulation for such fermions in the SF setup is a nontrivial task because SF boundary conditions break chiral symmetry explicitly. We will address this issue in the next section. However, Taniguchi [9] made the first attempt to formulate overlap fermions by using an orbifolding technique. Subsequently, he provided a formulation for domain-wall fermions [10], and then he and his collaborators [11] calculated a renormalized $B_{\mathrm{K}}$ in quenched QCD. Sint [12] developed such techniques by using a flavor twisting trick. However, these orbifolding formulations are constrained by the requirement that the number of flavors be even. Thus, apparently such formulations are incompatible with current trends toward dynamical three-flavor simulations. To overcome this difficulty, Lüscher [13] gave a completely different approach relying on a universality argument, dimensional power counting and symmetry considerations. Some perturbative calculations were performed in Ref. [14]. A crucial property of this formulation is that there is no restriction on the number of flavors. Since only overlap fermions were considered in Ref. [13], our main purpose here is to formulate the other chiral fermions, namely, domain-wall fermions.

The rest of the paper is organized as follows. Section II gives the formulation of domain-wall fermions in the SF setup, after a brief review of the universality argument. We present several pieces of numerical evidence in Secs. III and IV to show that our formulation is working properly. We also discuss the lattice artifacts for the step scaling function in Sec. V. In the last section, we conclude by giving some remarks and an outlook.

## II. FORMULATION

In the following, we assume that the reader is familiar with the SF in QCD [8,15]. After giving a brief reminder of the universality argument, we give a formulation for DWF and finally check the chiral symmetry breaking structure numerically.

### A. Universality argument

This subsection is a review of Lüscher's work in Ref. [13]. In the massless continuum theory, the Dirac operator $D$ satisfies the anticommutation relation with $\gamma_5$,

*Present address: Institute for Theoretical Physics, Kanazawa University, Kanazawa 920-1192, Japan.
takeda@hep.s.kanazawa-u.ac.jp

 

$$\gamma_5 D + D\gamma_5 = 0. \tag{1}$$

The above is true even in the SF setup, although the boundary conditions

$$P_+ \psi(x) = 0 \quad \text{at } x_0 = 0, \tag{2}$$

$$P_- \psi(x) = 0 \quad \text{at } x_0 = T, \tag{3}$$

with $P_\pm = (1 \pm \gamma_0)/2$, break chiral symmetry explicitly. Equation (1) means that the operator itself does not know about boundary conditions. In the continuum theory, information such as boundary conditions is embedded in the Hilbert space. In fact, the corresponding propagator, which is a solution of the inhomogeneous equation,

$$DS(x, y) = \delta(x - y), \tag{4}$$

fails to satisfy the anticommutation relation. Instead, it follows

$$\gamma_5 S(x, y) + S(x, y)\gamma_5 = \int_{z_0=0} d^3\mathbf{z} S(x, z)\gamma_5 P_- S(z, y) + \int_{z_0=T} d^3\mathbf{z} S(x, z)\gamma_5 P_+ S(z, y). \tag{5}$$

This can be derived by using partial integration on the SF manifold which has two boundaries at time slice $x_0 = 0$ and $T$. The nonvanishing right-hand side in Eq. (5) shows an explicit chiral symmetry breaking. Since such a breaking term is supported only on the time boundaries, the chiral symmetry is preserved in the bulk.

If someone naively tries to formulate chiral fermions on the lattice as discussed in Ref. [9], one may define an overlap operator, for example, with the Wilson kernel in the SF setup [15]. However, such an operator immediately satisfies the Ginsparg-Wilson (GW) relation and thus cannot reproduce Eq. (5) in the continuum limit. This indicates that such a naive formulation does not work and furthermore may belong to another boundary universality class, which is not what we want. In this way, it is a nontrivial task to formulate chiral fermions in the SF setup.

Some years ago, Lüscher [13] proposed a clever way to overcome this situation. First, consider the relation for the propagator in Eq. (5). This indicates that the GW relation has to be modified by boundary effects. Thus one has to find a modified overlap operator that breaks the GW relation near the time boundaries and correctly reproduces Eq. (5) in the continuum limit. Actually, finding such a modified operator is not so hard. However, a new question that naturally arises is how the SF boundary conditions emerge. For the Wilson fermion case [15], because there is a transfer matrix, it is natural for fermion fields to follow the SF boundary conditions. However, for chiral fermions, there is no such transfer matrix that can be defined from nearest neighbor interaction in the time direction. Therefore, it is not an easy task.

Lüscher [13] gave another point of view to see how fields respect the boundary condition. In the quantum field theory, the correlation function can tell us what kinds of boundary conditions are imposed. As an example, let us see how the boundary conditions emerge for Wilson fermions whose action is given by

$$S_{\mathrm{w}} = \sum_x \bar{\psi}(x) D_{\mathrm{w}}(m) \psi(x), \tag{6}$$

$$D_{\mathrm{w}}(m) = \frac{1}{2}\Big[\sum_\mu (\nabla_\mu + \nabla^*_\mu)\gamma_\mu - a\sum_\mu \nabla^*_\mu \nabla_\mu\Big] + m, \tag{7}$$

where $\nabla_\mu$ and $\nabla^*_\mu$ are forward and backward covariant difference operators, respectively,

$$\nabla_\mu \psi(x) = \frac{1}{a}[U(x, \mu)\psi(x + a\hat{\mu}) - \psi(x)], \tag{8}$$

$$\nabla^*_\mu \psi(x) = \frac{1}{a}[\psi(x) - U(x - a\hat{\mu}, \mu)^{-1}\psi(x - a\hat{\mu})]. \tag{9}$$

In the SF setup, the sum over $x$ in the action is a little bit subtle. We assume that the dynamical fields are $\psi(x)$ with $a \le x_0 \le T - a$, and the fields $\psi(x)$ with $x_0 \le 0$ and $T \le x_0$ are set to zero. For this setup, the propagator may be defined by

$$\langle \eta(x)\bar{\psi}(y)\rangle = a^{-4}\delta_{x,y}, \tag{10}$$

$$\eta(x) = \frac{\delta S_{\mathrm{w}}}{\delta \bar{\psi}(x)}. \tag{11}$$

For $2a \le x_0 \le T - 2a$, Eq. (11) becomes

$$\eta(x) = D_{\mathrm{w}}(m)\psi(x). \tag{12}$$

On the other hand, at $x_0 = a$, we obtain

$$\eta(x) = \frac{1}{a}P_+\psi(x) - \nabla_0 P_-\psi(x) + \frac{1}{2}\Big[\sum_k (\nabla_k + \nabla^*_k)\gamma_k - a\sum_k \nabla^*_k \nabla_k\Big]\psi(x) + m\psi(x). \tag{13}$$

By substituting Eq. (13) into Eq. (10) with $x \neq y$, we obtain

$$\frac{1}{a}P_+\langle\psi(x)\bar{\psi}(y)\rangle|_{x_0=a} - \nabla_0 P_-\langle\psi(x)\bar{\psi}(y)\rangle|_{x_0=a} + \cdots = 0. \tag{14}$$

In the continuum limit, the first term is dominant,

$$\frac{1}{a}P_+\langle\psi(x)\bar{\psi}(y)\rangle|_{x_0=0} = 0. \tag{15}$$

This shows that in the naive continuum limit, the Dirichlet-type boundary condition ($P_+\psi|_{x_0=0}=0$) is stable against the Neumann one ($\nabla_0 P_-\psi|_{x_0=0}=0$), and in the end the SF boundary conditions in Eq. (2) emerge. It is plausible that similar results are also obtained for the chiral fermions case, as long as the locality and symmetry are kept in a proper way, although we expect that the coefficient of the lowest dimensional operators ($\frac{1}{a}P_+\psi$) may be different from the case above, and additional higher dimensional terms may appear in Eq. (13). The important point here is that continuum SF boundary conditions emerge dynamically in the continuum limit of the correlation function. This boundary condition is natural and automatically guaranteed to emerge from the dimensional power-counting argument. Therefore, when we construct chiral fermions in the SF, we only have to prepare a modified operator by introducing an additional term that breaks the chiral symmetry near the time boundaries. Once this condition is fulfilled, then such an operator automatically becomes the desired one in the continuum limit without fine-tuning. A final important note is that the form of the boundary term is irrelevant as long as it will go into a preferred boundary universality class. Therefore, there is a large amount of freedom when choosing boundary terms, and one can use this freedom for practical purposes.

Following these guiding principles, Lüscher [13] proposed the operators

$$\bar{a}D_{\mathrm{N}} = 1 - \frac{1}{2}(U + \tilde{U}), \tag{16}$$

$$U = A(A^\dagger A + caP)^{-1/2}, \qquad \tilde{U} = \gamma_5 U^\dagger \gamma_5, \tag{17}$$

$$A = 1 + s - aD_{\mathrm{w}}(0), \qquad \bar{a} = a/(1+s), \tag{18}$$

with the parameter in the range $|s|<1$. $D_{\mathrm{w}}(0)$ is the massless Wilson operator in the SF. The key point here is the presence of the $P$ term in the inverse square root, which is given by

$$aP(x,y) = \delta_{\mathbf{x},\mathbf{y}}\delta_{x_0,y_0}(\delta_{x_0,a}P_- + \delta_{x_0,T-a}P_+). \tag{19}$$

Note that this term is supported near the time boundaries and thus called a boundary operator. The presence of this term breaks the GW relation explicitly, and the breaking is given by

$$\Delta_{\mathrm{B}} = \gamma_5 D_{\mathrm{N}} + D_{\mathrm{N}}\gamma_5 - \bar{a}D_{\mathrm{N}}\gamma_5 D_{\mathrm{N}}. \tag{20}$$

It was shown in Ref. [13] that this term is local and supported in the vicinity of the boundaries up to the exponentially small tails.

Although this operator breaks chiral symmetry explicitly, other symmetries (the discrete rotational symmetries in three dimensions, $C$, $P$ and $T$, flavor symmetry and so on) have to be maintained since the boundary conditions in Eqs. (2) and (3) are invariant under these symmetries. In addition, this operator has $\gamma_5$ Hermiticity. In this way, the universality-based formulation can avoid breaking important symmetries, such as the flavor symmetry. This is a distinctive feature of this formulation compared with the orbifolding technique, where flavor symmetries cannot be maintained or there is a constraint on the number of flavors.

Before leaving this subsection, let us summarize the guiding principles of formulating chiral fermions in the SF setup. What we learned from this construction is that, for an originally chiral fermion operator, one has to introduce an additional term to break the chiral symmetry and then demand that such breaking only appears near the time boundaries. Furthermore, one must maintain important symmetries as well as $\gamma_5$ Hermiticity. Once these conditions are fulfilled, it is automatically guaranteed that the lattice operator will correctly reproduce the continuum results according to the universality argument.

### B. Formulation of domain-wall fermions

Let us apply the guiding principles given in the previous subsection to domain-wall fermions. We propose a massless[1] domain-wall fermion action

$$S = a^4 \sum_{x,x'} \sum_{s,s'=1}^{L_s} \bar{\psi}(x,s)(D_{\mathrm{DWF}})_{xs,x's'}\psi(x',s'), \tag{21}$$

where a massless operator with $L_s = 6$, for example,[2] in four-dimensional block form is given by

$$aD_{\mathrm{DWF}} = \begin{bmatrix} a\tilde{D}_{\mathrm{w}} & -P_L & 0 & 0 & 0 & cB \\ -P_R & a\tilde{D}_{\mathrm{w}} & -P_L & 0 & cB & 0 \\ 0 & -P_R & a\tilde{D}_{\mathrm{w}} & -P_L + cB & 0 & 0 \\ 0 & 0 & -P_R - cB & a\tilde{D}_{\mathrm{w}} & -P_L & 0 \\ 0 & -cB & 0 & -P_R & a\tilde{D}_{\mathrm{w}} & -P_L \\ -cB & 0 & 0 & 0 & -P_R & a\tilde{D}_{\mathrm{w}} \end{bmatrix}, \tag{22}$$

with the chiral projections

[1]The mass term can be introduced in the usual way, namely, $a^4 m_{\mathrm{f}} \sum_{\mathbf{x}} \sum_{x_0=a}^{T-a} [\bar{\psi}(x,1)P_R\psi(x,L_s) + \bar{\psi}(x,L_s)P_L\psi(x,1)]$.

[2]We restrict ourselves to an even number of $L_s$, which is the case usually implemented.

$$P_{R/L} = (1 \pm \gamma_5)/2. \quad (23)$$

We also assume that the dynamical fields are $\psi(x, s)$ with $a \le x_0 \le T - a$. The block elements in Eq. (22) are four-dimensional operators, and $a\tilde{D}_{\mathrm{w}}$ is given by

$$a\tilde{D}_{\mathrm{w}} = aD_{\mathrm{w}}(-m_5) + 1. \quad (24)$$

The domain-wall height parameter usually takes a value in a range $0 < am_5 < 2$.

An important ingredient here is the presence of $B$ in Eq. (22) terms in the cross-diagonal elements. The reason for this $s$ dependence is to break the chiral symmetry in a similar way to the usual mass term [16]. As mentioned before, such chiral symmetry breaking should be present only near time boundaries; therefore, we choose the $B$ term as

$$B(x, y) = \delta_{\mathbf{x},\mathbf{y}}\delta_{x_0,y_0}\gamma_5(\delta_{x_0,a}P_- + \delta_{x_0,T-a}P_+), \quad (25)$$

which is supported near the boundaries. In this way, the time dependence is fixed. The spinor structure ($\gamma_5 P_\pm$) is determined by imposing the discrete symmetries $C$, $P$ and $T$ and $\Gamma_5$ Hermiticity. These requirements are not strong enough to determine the spinor structure completely, and therefore there is some freedom. The structure proposed here is only one of many solutions. Actually, we examined several choices of the spinor structure in the boundary term and confirmed numerically the universal results in the continuum limit for the lowest eigenvalue. In the following, we take this boundary term in Eq. (25).

The boundary coefficient $c$ is supposed to be nonzero to correctly reproduce the continuum theory, as we will see in Sec. III. It also plays an important role in canceling boundary $O(a)$ cutoff effects and has a perturbative expansion

$$c = c^{(0)} + c^{(1)}g_0^2 + O(g_0^4). \quad (26)$$

In the same way as in [14], which is based on enforcing an axial Ward-Takahashi identity at tree level, we tune the first coefficient $c^{(0)}$ as a function of the domain-wall height $am_5$,

$$c^{(0)} = 0.5089 - 0.0067(am_5 - 1) + 0.0488(am_5 - 1)^2 - 0.0216(am_5 - 1)^3 + 0.0673(am_5 - 1)^4. \quad (27)$$

This is valid in the region where the bulk $O(a)$ can be neglected,[3] that is, for sufficiently large $L_s$. In the process of this determination, one needs to define the operators of the axial vector current and pseudoscalar density. We give their definition together with that of the conserved axial current in Appendix A 3.

[3]Actually, we observe that $O(a)$ improvement does not work for small $L_s$ and values of $am_5$ that are far from 1. For example, $O(a)$ terms in $f_A$ and $f_P$ (defined in Appendix A 3) at tree level do not vanish simultaneously with the same value of $c^{(0)}$.

### C. Structure of chiral symmetry breaking at tree level

In this subsection, let us check the important properties of the operator defined in the previous section. A reader may worry that, even though the additional boundary term is localized to the time boundary, after integrating over the fifth-dimensional degree of freedom, such breaking effects may leak into the four-dimensional bulk and ruin the bulk chiral symmetry. To settle this question, we numerically investigate the structure of chiral symmetry breaking by looking at the breaking of the GW relation

$$\Delta^{(L_s)} = \gamma_5 D_{\mathrm{eff}}^{(L_s)} + D_{\mathrm{eff}}^{(L_s)}\gamma_5 - 2aD_{\mathrm{eff}}^{(L_s)}\gamma_5 D_{\mathrm{eff}}^{(L_s)}, \quad (28)$$

with the effective four-dimensional operator [17,18]

$$\det D_{\mathrm{eff}}^{(L_s)} = \det[D_{\mathrm{DWF}}/D_{\mathrm{PV}}]. \quad (29)$$

The Pauli-Villars (PV) operator is defined as the massive DWF operator with $am_{\mathrm{f}} = -1$. To obtain the effective operator, first of all, we have to define physical quark fields,

$$q(x) = P_L\psi(x, 1) + P_R\psi(x, L_s), \quad (30)$$

$$\bar{q}(x) = \bar{\psi}(x, 1)P_R + \bar{\psi}(x, L_s)P_L. \quad (31)$$

In terms of the propagator of domain-wall fermions defined by

$$D_{\mathrm{DWF}}S_{\mathrm{DWF}}(x, y; s, t) = a^{-4}\delta_{x,y}\delta_{s,t}, \quad (32)$$

that of the physical field is expressed as

$$\begin{aligned}[q(x)\bar{q}(y)]_{\mathrm{F}} &= S_{\mathrm{q}}(x, y) \\ &= P_L S_{\mathrm{DWF}}(x, y; 1, L_s)P_L + P_L S_{\mathrm{DWF}}(x, y; 1, 1)P_R \\ &\quad + P_R S_{\mathrm{DWF}}(x, y; L_s, L_s)P_L \\ &\quad + P_R S_{\mathrm{DWF}}(x, y; L_s, 1)P_R. \end{aligned} \quad (33)$$

In terms of $S_{\mathrm{q}}$ the effective operator is given by

$$aD_{\mathrm{eff}}^{(L_s)} = (1 + a^3 S_{\mathrm{q}})^{-1}. \quad (34)$$

In the SF setup, $\Delta^{(L_s)}$ in Eq. (28) contains not only bulk chiral symmetry breaking but also boundary breaking. The former is supposed to be removed by taking $L_s$ to infinity. In such a limit, boundary breaking effects remain and they are expected to be localized near the time boundaries. To see this situation, we numerically compute $\Delta^{(L_s)}$ for a free operator. In the free case, we can perform the Fourier transformation for spatial directions. We study the momentum configuration $\mathbf{p} = (0, 0, 0)$ in the following. The remaining dimensions are only the time direction and spinor space; therefore, for a given $L_s$ and a fixed spatial momentum configuration, $\Delta^{(L_s)}$ is a matrix with dimension $4(T/a - 1)$. Figure 1 shows the magnitude of $\ln(\|\Delta^{(L_s)}(x_0, y_0)\|_{\mathrm{spin}})$, where the norm is taken for the

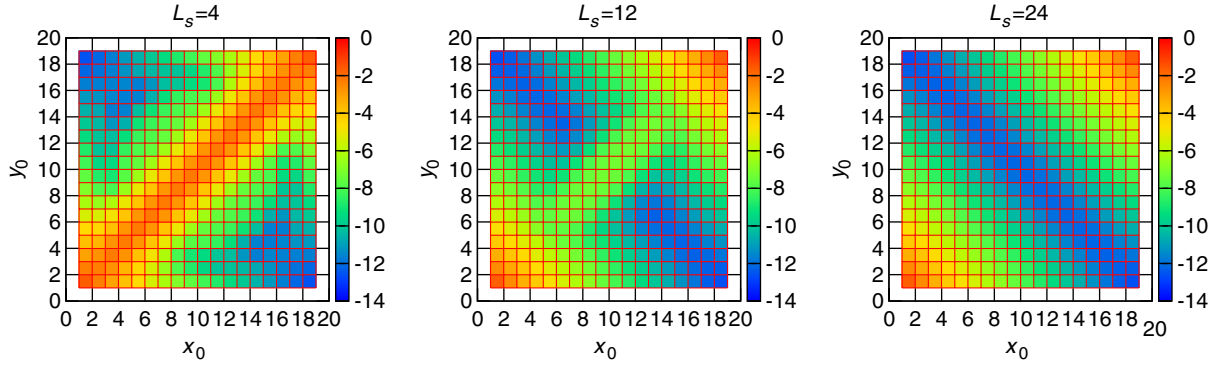


FIG. 1 (color online). The color range $[-14, 0]$ corresponds to the value of $\ln \|\Delta^{(L_s)}(x_0, y_0)\|_{\text{spin}}$ for the zero spatial momentum configuration with the parameters $T/a = 20$, $m_f = 0$, $am_5 = 1$ and $c = 1$.

spinor space only. By increasing $L_s$, bulk symmetry breaking is reduced. Finally, at $L_s = 24$, only boundary breaking effects remain and they are localized exponentially near the time boundaries. This is the expected behavior for overlap fermions [13]. We conclude that the presence of the boundary term causes chiral symmetry breaking, which decays exponentially away from the time boundaries for the effective four-dimensional operator.

## III. SPECTRUM OF A FREE OPERATOR

In this section, we investigate the free spectrum of the DWF operator to confirm universality at tree level. We set $T = L$ in this section.

### A. Spectrum of $D^\dagger_{\text{DWF}} D_{\text{DWF}}$

To achieve better chiral symmetry, the (physical) eigenmodes of the domain-wall operator should be localized near the boundaries of the fifth direction and propagate in the space-time directions. This should also be true in the SF setup, since the chiral symmetry is supposed to be maintained in the bulk. To observe such phenomena, we numerically compute the lowest eigenmode of the operator $D^\dagger_{\text{DWF}} D_{\text{DWF}}$ with the trivial gauge configuration $U(x, \mu) = 1$. In the free case, we can perform the Fourier transformation for spatial directions and project out the momentum configuration $\mathbf{p} = (0, 0, 0)$. Thus, remaining indices of the vector space are now the spinor, the time $x_0$ and the extra dimension $s$,

$$D^\dagger_{\text{DWF}} D_{\text{DWF}} \psi(x_0, s) = \lambda \psi(x_0, s), \tag{35}$$

where the spinor indices are suppressed. We set input parameters $am_5 = 1$ and $\theta = 0$. $\theta$ is the parameter that controls the spatial boundary condition for fermion fields. (For more details, we refer to [19].)

We numerically compute the lowest eigenvalue and the corresponding eigenfunction $\|\psi(x_0, s)\|_{\text{spin}}$. We examine not only the case $c = 1$ but also $c = 0$ to investigate the importance of the presence of the boundary operator. The scaling behavior of the eigenvalue is shown in Fig. 2. For $c = 1$, $L_s$ dependence is too small to see on this scale. The lowest eigenvalues properly converge to their continuum values; therefore, universality is confirmed. Furthermore, the associated eigenfunction shows nice localization behavior, namely, being localized for the fifth direction and propagating for the time direction, as shown in the left panel of Fig. 3, revealing that this mode is a physical one.

For $c = 0$ in Fig. 2, although all $L_s = 4$, 16, 32 results tend to converge to the continuum limit, large $L_s$ results have a bending phenomenon in the small $a/L$ region and show no power decay in terms of $a/L$. This indicates that if one takes $L_s$ to infinity before taking the $a/L = 0$ limit, the eigenvalue will likely converge to zero. If this is so, the theory with $L_s = \infty$ does not belong to the correct universality class. Furthermore, the eigenfunction in the right panel in Fig. 3 is localized on the edges in the time-$s$ plane. This is a typical unphysical mode. On the other hand, interestingly, for small $L_s$, the scaling behavior is rather mild. In the small $L_s$ case, the chiral symmetry breaking of domain-wall fermions is rather similar to that of the ordinary Wilson fermions. As in the Wilson fermion case, the

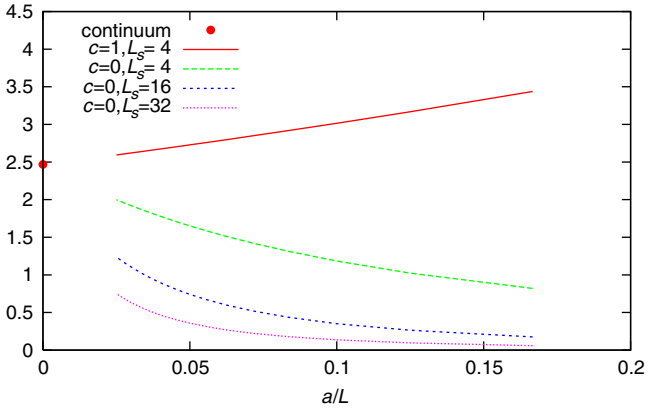


FIG. 2 (color online). The lowest eigenvalue of $L^2 D^\dagger_{\text{DWF}} D_{\text{DWF}}$ with $am_5 = 1$. Some combinations of parameters $c$ and $L_s$ are shown. The continuum value is $\pi^2/4 = 2.467\ldots$. For $c = 1$, since the $L_s$ dependence is so weak on this scale, we show only $L_s = 4$ results.

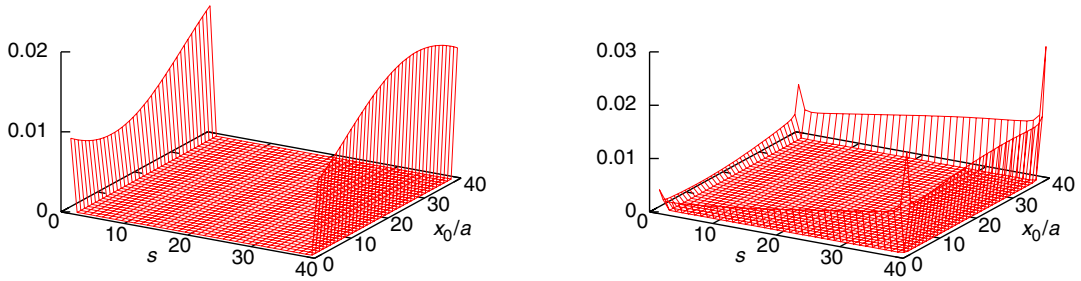


FIG. 3 (color online). $\|\psi(x_0, s)\|_{\text{spin}}$ with zero spatial momentum and the parameters $T/a = L_s = 40$, $\theta = 0$ and $am_5 = 1$. The norm for the eigenvector is taken in the spinor space. The left (right) panel is for $c = 1$ ($c = 0$).

bulk chiral symmetry breaking for DWFs due to finite $L_s$ plays some role in producing the correct continuum limit. This is the reason why DWFs with smaller $L_s$ and no boundary term $B$ can produce the continuum results.

The results in this subsection show that the boundary term with $c \neq 0$ plays an important role in putting the theory in the correct universality class.

### B. Spectrum of $D_{\text{q}}^{\dagger} D_{\text{q}}$

Not all eigenmodes of $D_{\text{DWF}}$ are physical ones, and how to eliminate the unphysical mode is not clear. To extract physical modes only, let us study the eigenmodes of $D_{\text{q}}$, where unphysical modes are excluded. The operator $D_{\text{q}}$ is defined from $S_{\text{q}}$ in Eq. (33),

$$D_{\text{q}} S_{\text{q}}(x, y) = a^{-4} \delta_{x,y}. \tag{36}$$

We numerically compute the lowest ten eigenvalues of $D_{\text{q}}^{\dagger} D_{\text{q}}$ with the parameter set to $am_5 = 1$, $\theta = 0$, $\pi/5$ and $c = 1$ in the presence of the background gauge field (choice A in Ref. [20]). The values obtained for $L/a = T/a = 6, 12, 24$ are summarized in Table I. All tables are given in Appendix B. The scaling behavior of the eigenvalues is shown in Fig. 4. Although we show two cases of $L_s$, namely, $L_s = 4$ and $L_s = 32$, it is hard to see the difference on this scale. We observe that they converge to the continuum values given in Ref. [19]. This behavior persists for a variety of values of $c$, $0.5 \leq c \leq 1.5$. This result confirms the universality at tree level.

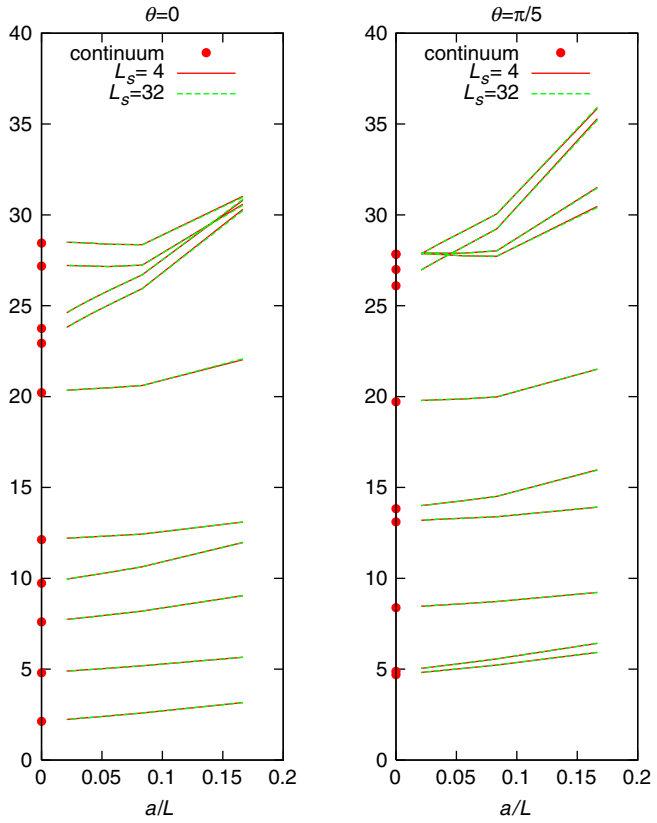


FIG. 4 (color online). The $a/L$ dependence of the lowest ten eigenvalues of $L^2 D_{\text{q}}^{\dagger} D_{\text{q}}$ in the presence of the background gauge field. The left (right) panel is for $\theta = 0$ ($\theta = \pi/5$). The parameters are set to $am_5 = 1$ and $c = 1$. The red points at $a/L = 0$ are continuum values [19].

## IV. ONE-LOOP ANALYSIS OF SF COUPLING

To further check the universality at the quantum level as well as the renormalizability, we perform the one-loop-order calculation of the SF coupling.

### A. Definition and results

We compute the fermion contribution to the SF coupling [19] $p_{1,1}(L/a, L_s)$ (we set $L = T$ as usual) at one-loop order for massless domain-wall fermions. The one-loop coefficient is given as

$$p_{1,1}(L/a, L_s) = \frac{1}{k} \frac{\partial}{\partial \eta} \ln \det (D_{\text{DWF}}/D_{\text{PV}})|_{\eta=\nu=0}, \tag{37}$$

with the normalization (see [19] for details)

$$k = 12(L/a)^2[\sin(\gamma) + \sin(2\gamma)], \qquad \gamma = \frac{1}{3}\pi(a/L)^2. \tag{38}$$

The parameters $\eta$ and $\nu$ parametrize the background gauge field [20]. In the actual calculation, we expand the $\eta$ derivative and use the fact that the determinant is factorized for individual spatial momentum $\mathbf{p}$ and color sector $b$,

$$p_{1,1}(L/a, L_s) = \frac{1}{k}\,\mathrm{Tr}\left[ D_{\mathrm{DWF}}^{-1}\frac{\partial D_{\mathrm{DWF}}}{\partial \eta} - D_{\mathrm{PV}}^{-1}\frac{\partial D_{\mathrm{PV}}}{\partial \eta}\right]$$
$$= \frac{1}{k}\sum_{\mathbf{p}}\sum_{b=1}^{3}\mathrm{tr}\left[ (D^b_{\mathrm{DWF}})^{-1}(\mathbf{p})\frac{\partial D^b_{\mathrm{DWF}}(\mathbf{p})}{\partial \eta} - (D^b_{\mathrm{PV}})^{-1}(\mathbf{p})\frac{\partial D^b_{\mathrm{PV}}(\mathbf{p})}{\partial \eta}\right]. \quad (39)$$

The trace tr concerns the spinor, the time indices and the fifth coordinate only. It may be worthwhile to note that for our definition of DWF,

$$\frac{\partial D_{\mathrm{DWF}}}{\partial \eta} = \frac{\partial D_{\mathrm{PV}}}{\partial \eta} \quad (40)$$

holds since the mass term does not involve the gauge field.

We compute $p_{1,1}$ on the lattices of size $L/a = 4, 6, \ldots, 48$ and $L_s = 6,\ 8,\ 10,\ 12,\ 16$ with parameters $0.7 \le am_5 \le 1.3$ and $\theta = \pi/5$. Subsets of the results are summarized in Table II for $am_5 = 1$, $L_s = 6$ and $L/a = 4, 6, \ldots, 48$. Separate contributions from DWF and PV are also shown there.

### B. Coefficients of Symanzik's expansion

From Symanzik's analysis of the cutoff dependence of Feynman diagrams on the lattice, one expects that the one-loop coefficient has an asymptotic expansion in terms of $a/L$,

$$p_{1,1}(L/a, L_s) = \sum_{n=0}^{\infty}(a/L)^n[A_n(L_s) + B_n(L_s)\ln(L/a)]. \quad (41)$$

Note that the coefficients $A_n$ and $B_n$ $(n = 0, 1, 2, \ldots)$ depend on $L_s$. We can reliably extract the first few coefficients by making use of the method described in Ref. [21].

For the usual renormalization of the coupling constant, $B_0$ at $L_s = \infty$ should be $2b_{0,1}$, where $b_{0,1}$ is the fermion part of the one-loop coefficient of the $\beta$ function for $N_{\mathrm{f}}$ flavors of QCD,

$$b_0 = b_{0,0} + N_{\mathrm{f}} b_{0,1}, \quad (42)$$

$$b_{0,0} = \frac{11}{(4\pi)^2}, \quad (43)$$

$$b_{0,1} = -\frac{2}{3}\frac{1}{(4\pi)^2}. \quad (44)$$

We confirmed that $B_0(L_s)$ for large $L_s$ (say, $L_s = 16$) converges to $2b_{0,1} = -0.008443\ldots$ up to three significant digits for the values of $am_5$ that we investigated. When the tree-level $O(a)$ improvement is realized, we expect that $B_1 = 0$ holds. We check this to $10^{-3}$ for the same parameter region as before. This shows that the formula for the boundary coefficient in Eq. (27) works well to achieve the tree-level $O(a)$ improvement to the precision considered here. In the following analysis, we set exact values $B_0 = 2b_{0,1} = -1/(12\pi^2)$ and $B_1 = 0$.

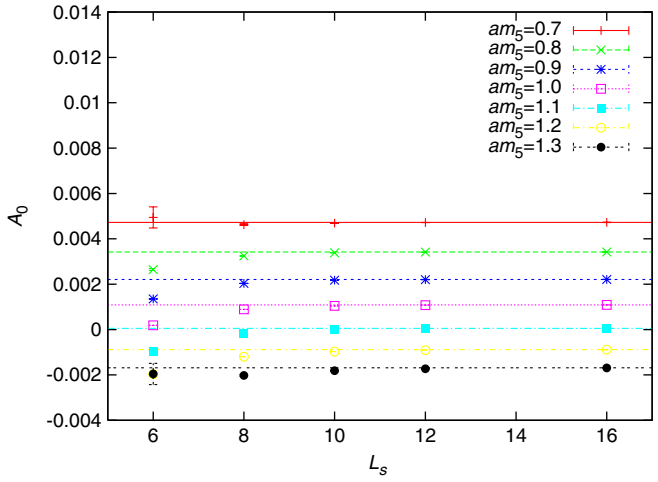


FIG. 5 (color online). $L_s$ dependence of $A_0$ for $0.7 \le am_5 \le 1.3$. The horizontal lines show the values of $A_0$ in the infinity $L_s$ limit, which are obtained by combining the results of the previous literature [19,22].

$A_0$ gives information about a ratio of $\Lambda$ parameters. The obtained values of $A_0(L_s)$ as a function of $L_s$ are shown in Fig. 5. By combining the previous results from Refs. [19,22], the values of $A_0$ at infinity $L_s$ can be obtained and are shown in Fig. 5 as the horizontal lines. We observe that our results at finite $L_s$ properly converge to the known results at infinity $L_s$.

To achieve one-loop $O(a)$ improvement, we need to determine the coefficient of the fermion part of the boundary counterterm $c_{\mathrm{t}}^{(1,1)}$ [19] at one-loop order. If one imposes an improvement condition [19], one finds that

$$c_{\mathrm{t}}^{(1,1)} = A_1/2. \quad (45)$$

Therefore, we need the value of $A_1$. The obtained values of $A_1$ are given in Table III. For future reference, we provide an interpolation formula for $c_{\mathrm{t}}^{(1,1)}$ as a polynomial of $am_5$ for larger $L_s$, where the value of $A_1$ is saturated,

$$c_{\mathrm{t}}^{(1,1)} = 0.00434 + 0.01102(am_5 - 1) - 0.00858(am_5 - 1)^2, \quad (46)$$

for $0.7 \le am_5 \le 1.3$.

## V. LATTICE ARTIFACTS OF THE STEP SCALING FUNCTION TO ONE-LOOP ORDER

In this section, we investigate lattice artifacts of the step scaling function [23] $\sigma(2, u)$, which describes the evolution of the running coupling $\bar{g}^2(L) = u$ under changes of scale $L$ by a factor 2,

$$\sigma(2, u) = \bar{g}^2(2L), \qquad u = \bar{g}^2(L). \tag{47}$$

The lattice version of the step scaling function is denoted by $\Sigma(2, u, a/L)$, which contains lattice artifacts. Such lattice artifacts are described by the relative deviation

$$\delta(u, a/L) \equiv \frac{\Sigma(2, u, a/L) - \sigma(2, u)}{\sigma(2, u)}. \tag{48}$$

By expanding the relative deviation in terms of the coupling constant $u$, one obtains

$$\delta(u, a/L) = \delta_1(a/L)u + O(u^2), \tag{49}$$

where the one-loop deviation $\delta_1(s, a/L)$ may be decomposed into a pure gauge and a fermion part [19],

$$\delta_1(a/L) = \delta_{1,0}(a/L) + N_f\delta_{1,1}(a/L). \tag{50}$$

We are currently only interested in the fermion part. We consider domain-wall fermions; thus, the fermion part of the one-loop deviation $\delta_{1,1}(a/L, L_s)$ contains $L_s$ dependence. In terms of the one-loop coefficient of the SF coupling $p_{1,1}$, the one-loop deviation is given by

$$\delta_{1,1}(a/L, L_s) = p_{1,1}(2L/a, L_s) - p_{1,1}(L/a, L_s) - 2b_{0,1}\ln(2). \tag{51}$$

Depending on the value of the boundary counterterm $c_t^{(1,1)}$, we denote by $\delta_{1,1}^{(0)}$ the tree-level $O(a)$ improved version with $c_t^{(1,1)} = 0$, and by $\delta_{1,1}^{(1)}$ the one-loop $O(a)$ improved one for $c_t^{(1,1)}$ in Eq. (45).

We show numerical results for the one-loop deviation in Tables IV and V and Fig. 6, where we include those of the Wilson-type fermions [19] and overlap fermions [14] for comparison. The $L_s$ dependence of the DWFs is small. In the case of the clover action, $c_t^{(1,1)}$ is set to be the proper value to achieve one-loop $O(a)$ improvement, and for Wilson fermions it is set to $c_t^{(1,1)} = 0$. We observe that the lattice artifacts for domain-wall fermions are small for the case of tree-level boundary $O(a)$ improvement compared with other fermions, while they are large for the case of one-loop boundary $O(a)$ improvement.

## VI. CONCLUSION AND OUTLOOK

In this paper, we provide a new formulation of domain-wall fermions in the SF setup by following the universality argument of Lüscher. In contrast to the previous formulation by Taniguchi, ours can deal with the boundary $O(a)$ improvement properly, and there is no constraint on the number of flavors. To check that our formulation works properly, we investigate the spectrum and eigenmodes of the free operator and perform a one-loop analysis of the SF coupling constant. Then we confirm the universality at tree level and one-loop level and observe that all results investigated show the desired behaviors.

Before starting simulations, the boundary improvement coefficient $c$ should be determined to one-loop order. This involves calculations of the SF correlators, $f_A$, $f_P$, etc., given in Appendix A. These calculations could be performed in a way similar to the case of the Wilson fermion.

As mentioned before, one of the most important properties of the universality-based formulation is that there are no restrictions to the number of flavors. By taking advantage of this property, we may compute the renormalization factor of $B_K$ for $N_f = 3$ QCD.

## ACKNOWLEDGMENTS

We would like to thank Sinya Aoki, Yasumichi Aoki, Norman Christ, Michael Endres, Taku Izubuchi,

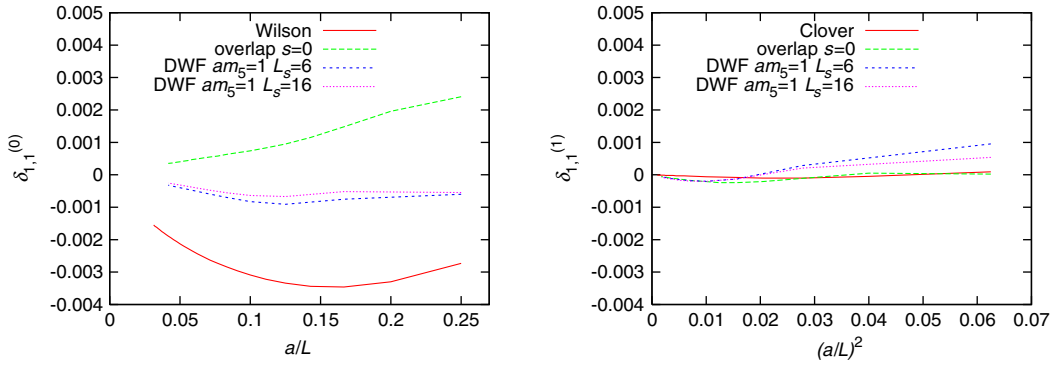


FIG. 6 (color online). The relative deviations with the various actions for tree-level $O(a)$ improvement $\delta_{1,1}^{(0)}$ (left panel) and one-loop $O(a)$ improvement $\delta_{1,1}^{(1)}$ (right panel), for $\theta = \pi/5$ as a function of $a/L$ and $(a/L)^2$, respectively. For comparison, those of the Wilson-type fermion with $c_t^{(1,1)} = 0$ and the clover fermion with $c_t^{(1,1)} = 0.019141$ [19] are included in the plot of $\delta_{1,1}^{(0)}$ and $\delta_{1,1}^{(1)}$, respectively.

Changhoan Kim, Robert Mawhinney and the members of the RBC Collaboration for helpful discussions. We are grateful to Stefan Sint for his hospitality during our stay at Trinity College in Dublin, where this work was initiated. This work is supported by the U.S. Department of Energy under Grant No. DE-FG02-92ER40699.

## APPENDIX A: FERMION CORRELATORS

In this appendix, I summarize the fermion correlators, the boundary fields and so on that are often used in the SF setup.

### 1. Boundary fields

As given in Ref. [13], the lattice versions of the fermion boundary fields are defined as

$$\zeta(\mathbf{x}) = U(x - a\hat{0}, 0)P_- q(x)|_{x_0=a}, \tag{A1}$$

$$\bar{\zeta}(\mathbf{x}) = \bar{q}(x)P_+ U(x - a\hat{0}, 0)^{-1}|_{x_0=a}, \tag{A2}$$

$$\zeta'(\mathbf{x}) = U(x, 0)^{-1}P_+ q(x)|_{x_0=T-a}, \tag{A3}$$

$$\bar{\zeta}'(\mathbf{x}) = \bar{q}(x)P_- U(x, 0)|_{x_0=T-a}. \tag{A4}$$

Here, note that we use the physical quark fields defined in Eqs. (30) and (31).

### 2. Propagators

The propagators for the physical quark fields and the boundary fields are given by

$$[q(x)\bar{q}(y)]_{\mathrm{F}} = S_{\mathrm{q}}(x, y), \tag{A5}$$

$$[q(x)\bar{\zeta}(\mathbf{y})]_{\mathrm{F}} = S_{\mathrm{q}}(x, y)U(y - a\hat{0}, 0)^{-1}P_+|_{y_0=a}, \tag{A6}$$

$$[q(x)\bar{\zeta}'(\mathbf{y})]_{\mathrm{F}} = S_{\mathrm{q}}(x, y)U(y, 0)P_-|_{y_0=T-a}, \tag{A7}$$

$$[\zeta(\mathbf{x})\bar{q}(y)]_{\mathrm{F}} = P_- U(x - a\hat{0}, 0)S_{\mathrm{q}}(x, y)|_{x_0=a}, \tag{A8}$$

$$[\zeta'(\mathbf{x})\bar{q}(y)]_{\mathrm{F}} = P_+ U(x, 0)^{-1}S_{\mathrm{q}}(x, y)|_{x_0=T-a}, \tag{A9}$$

$$[\zeta(\mathbf{x})\bar{\zeta}'(\mathbf{y})]_{\mathrm{F}} = P_- U(x - a\hat{0}, 0)S_{\mathrm{q}}(x, y) \times U(y, 0)P_-|_{x_0=a,y_0=T-a}, \tag{A10}$$

$$[\zeta'(\mathbf{x})\bar{\zeta}(\mathbf{y})]_{\mathrm{F}} = P_+ U(x, 0)^{-1}S_{\mathrm{q}}(x, y) \times U(y - a\hat{0}, 0)^{-1}P_-|_{x_0=T-a,y_0=a}. \tag{A11}$$

### 3. Operators

We consider the degenerate quark mass case, and an extension to the flavor space is done in a trivial way. In terms of the physical quark fields, the local operators are defined as

$$A_\mu^a(x) = \bar{q}(x)\gamma_\mu\gamma_5\frac{1}{2}\tau^a q(x), \tag{A12}$$

$$P^a(x) = \bar{q}(x)\gamma_5\frac{1}{2}\tau^a q(x). \tag{A13}$$

The conserved axial vector current is given by

$$\mathcal{A}_\mu^a(x) = \sum_{s=1}^{L_s} \mathrm{sign}\left(s - \frac{L_s + 1}{2}\right) j_\mu^a(x, s), \tag{A14}$$

where

$$j_\mu^a(x, s) = \bar{\psi}(x + a\hat{\mu}, s)P_+^{(\mu)}U(x, \mu)^{-1}\frac{1}{2}\tau^a\psi(x, s) - \bar{\psi}(x, s)P_-^{(\mu)}U(x, \mu)\frac{1}{2}\tau^a\psi(x + a\hat{\mu}, s), \tag{A15}$$

with $P_\pm^{(\mu)} = (1 \pm \gamma_\mu)/2$.

### 4. Correlators

The fermion correlators for the local operators in the SF are given by

$$f_{\mathrm{A}}(x_0) = -a^6\sum_{a=1}^{N_{\mathrm{f}}}\sum_{\mathbf{y},\mathbf{z}}\frac{1}{N_{\mathrm{f}}^2 - 1}\left\langle A_0^a(x)\bar{\zeta}(\mathbf{y})\gamma_5\frac{1}{2}\tau^a\zeta(\mathbf{z})\right\rangle, \tag{A16}$$

$$f_{\mathrm{P}}(x_0) = -a^6\sum_{a=1}^{N_{\mathrm{f}}}\sum_{\mathbf{y},\mathbf{z}}\frac{1}{N_{\mathrm{f}}^2 - 1}\left\langle P^a(x)\bar{\zeta}(\mathbf{y})\gamma_5\frac{1}{2}\tau^a\zeta(\mathbf{z})\right\rangle, \tag{A17}$$

$$f_1 = -\frac{a^{12}}{L^6}\sum_{a=1}^{N_{\mathrm{f}}}\sum_{\mathbf{u},\mathbf{v},\mathbf{y},\mathbf{z}}\frac{1}{N_{\mathrm{f}}^2 - 1} \times\left\langle\bar{\zeta}'(\mathbf{u})\gamma_5\frac{1}{2}\tau^a\zeta'(\mathbf{v})\bar{\zeta}(\mathbf{y})\gamma_5\frac{1}{2}\tau^a\zeta(\mathbf{z})\right\rangle. \tag{A18}$$

After Wick contraction, they become

$$f_{\mathrm{A}}(x_0) = a^6\sum_{\mathbf{y},\mathbf{z}}\frac{1}{2}\langle[\zeta(\mathbf{z})\bar{q}(x)]_{\mathrm{F}}\gamma_0\gamma_5[q(x)\bar{\zeta}(\mathbf{y})]\gamma_5\rangle, \tag{A19}$$

$$f_{\mathrm{P}}(x_0) = a^6\sum_{\mathbf{y},\mathbf{z}}\frac{1}{2}\langle[\zeta(\mathbf{z})\bar{q}(x)]_{\mathrm{F}}\gamma_5[q(x)\bar{\zeta}(\mathbf{y})]\gamma_5\rangle, \tag{A20}$$

$$f_1 = \frac{a^{12}}{L^6}\sum_{\mathbf{u},\mathbf{v},\mathbf{y},\mathbf{z}}\frac{1}{2}\langle[\zeta(\mathbf{z})\bar{\zeta}'(\mathbf{u})]_{\mathrm{F}}\gamma_5[\zeta'(\mathbf{v})\bar{\zeta}(\mathbf{y})]_{\mathrm{F}}\gamma_5\rangle, \tag{A21}$$

where the propagators are given in Appendix A 2 and we have used

$$\sum_{a=1}^{N_f} \mathrm{tr}\left[\left(\frac{\tau^a}{2}\right)^2\right] = \frac{N_f^2-1}{2}. \tag{A22}$$

These correlators are the same as those of Wilson fermions except that the propagators are replaced by those of the physical quark field $S_q$.

For the conserved axial vector current, a correlator is given by

$$f_{\mathcal{A}}(x_0) = -a^6 \sum_{a=1}^{N_f} \sum_{\mathbf{y},\mathbf{z}} \frac{1}{N_f^2-1} \left\langle \mathcal{A}_0^a(x) \bar{\zeta}(\mathbf{y}) \gamma_5 \frac{1}{2} \tau^a \zeta(\mathbf{z}) \right\rangle. \tag{A23}$$

As an example, at tree level, this can be expressed in terms of the propagator for domain-wall fermions as

$$\begin{aligned} f_{\mathcal{A}}(x_0)|_{U=1} = \sum_{s=1}^{L_s} \mathrm{sign}\left(s - \frac{L_s+1}{2}\right) \frac{1}{2} \mathrm{Tr}[ & -P_+ S_{\mathrm{DWF}}(x,y;s,1)\gamma_0 P_L S_{\mathrm{DWF}}(y, x+a\hat{0};1,s) \\ & + P_- S_{\mathrm{DWF}}(x+a\hat{0},y;s,1)\gamma_0 P_L S_{\mathrm{DWF}}(y,x;1,s) + P_+ S_{\mathrm{DWF}}(x,y;s,1) P_R S_{\mathrm{DWF}}(y,x+a\hat{0};L_s,s) \\ & - P_- S_{\mathrm{DWF}}(x+a\hat{0},y;s,1) P_R S_{\mathrm{DWF}}(y,x;L_s,s) - P_+ S_{\mathrm{DWF}}(x,y;s,L_s) P_L S_{\mathrm{DWF}}(y,x+a\hat{0};1,s) \\ & + P_- S_{\mathrm{DWF}}(x+a\hat{0},y;s,L_s) P_L S_{\mathrm{DWF}}(y,x;1,s) + P_+ S_{\mathrm{DWF}}(x,y;s,L_s)\gamma_0 P_R S_{\mathrm{DWF}}(y,x+a\hat{0};L_s,s) \\ & - P_- S_{\mathrm{DWF}}(x+a\hat{0},y;s,L_s)\gamma_0 P_R S_{\mathrm{DWF}}(y,x;L_s,s)]. \end{aligned} \tag{A24}$$

## APPENDIX B: TABLES OF NUMERICAL RESULTS

TABLE I. The lowest ten eigenvalues of the Hermitian operator $L^2 D_q^\dagger D_q$ for $L_s = 4$, 32. The upper (lower) panel is for $\theta = 0$ ($\theta = \pi/5$). $b$ represents the color sector, and $d$ is the degeneracy for one flavor.

| | $L/a = 6$ | | $L/a = 12$ | | $L/a = 24$ | | | |
|---|---|---|---|---|---|---|---|---|
| $n$ | $L_s = 4$ | $L_s = 32$ | $L_s = 4$ | $L_s = 32$ | $L_s = 4$ | $L_s = 32$ | $b$ | $d$ |
| | | | | $\theta = 0$ | | | | |
| 1 | 3.161141 | 3.160760 | 2.591269 | 2.591267 | 2.350053 | 2.350053 | 2 | 2 |
| 2 | 5.658392 | 5.658925 | 5.191148 | 5.191161 | 4.990293 | 4.990293 | 2 | 2 |
| 3 | 9.050173 | 9.045312 | 8.196497 | 8.196424 | 7.888424 | 7.888424 | 3 | 2 |
| 4 | 11.981137 | 11.963010 | 10.635061 | 10.634737 | 10.177881 | 10.177878 | 1 | 2 |
| 5 | 13.098016 | 13.101850 | 12.434736 | 12.434839 | 12.281233 | 12.281235 | 3 | 2 |
| 6 | 22.037107 | 22.078353 | 20.612026 | 20.613136 | 20.436083 | 20.436098 | 1 | 2 |
| 7 | 30.304338 | 30.232012 | 25.944369 | 25.942289 | 24.578258 | 24.578235 | 2 | 2 |
| 8 | 30.810696 | 30.865401 | 26.708727 | 26.709232 | 25.378691 | 25.378700 | 2 | 2 |
| 9 | 30.585955 | 30.530965 | 27.241272 | 27.239584 | 27.184415 | 27.184395 | 1 | 6 |
| 10 | 31.026393 | 30.978110 | 28.357563 | 28.355829 | 28.438888 | 28.438866 | 3 | 6 |
| | | | | $\theta = \pi/5$ | | | | |
| 1 | 5.924559 | 5.922886 | 5.232916 | 5.232896 | 4.952553 | 4.952553 | 2 | 2 |
| 2 | 6.428276 | 6.423570 | 5.566868 | 5.566810 | 5.214696 | 5.214695 | 1 | 2 |
| 3 | 9.221621 | 9.223322 | 8.721989 | 8.722031 | 8.548948 | 8.548949 | 2 | 2 |
| 4 | 13.912656 | 13.926143 | 13.392223 | 13.392552 | 13.267533 | 13.267537 | 1 | 2 |
| 5 | 15.970852 | 15.951467 | 14.513964 | 14.513548 | 14.162258 | 14.162253 | 3 | 2 |
| 6 | 21.508691 | 21.520321 | 19.983404 | 19.983750 | 19.838031 | 19.838036 | 3 | 2 |
| 7 | 35.296282 | 35.214384 | 29.231042 | 29.228128 | 27.743584 | 27.743548 | 2 | 2 |
| 8 | 35.861910 | 35.932144 | 30.057783 | 30.058382 | 28.612335 | 28.612346 | 2 | 2 |
| 9 | 30.468452 | 30.406862 | 27.727188 | 27.725168 | 27.806412 | 27.806386 | 1 | 6 |
| 10 | 31.520474 | 31.475867 | 28.021244 | 28.019681 | 27.896264 | 27.896245 | 3 | 6 |

TABLE II. The one-loop coefficient of the SF coupling $p_{1,1}(L/a, L_s)$ with $L_s = 6$, $am_5 = 1$ and $\theta = \pi/5$. In Eq. (39), there are two sources of contributions: DWF and PV, which are shown separately in the table.

| $L/a$ | $p_{1,1}(L/a, 6)$ | DWF contribution | PV contribution |
|---|---|---|---|
| 4 | −0.0090558230 | −0.0463742376 | −0.0373184146 |
| 6 | −0.0128831139 | −0.0614487481 | −0.0485656342 |
| 8 | −0.0155107254 | −0.0717039592 | −0.0561932338 |
| 10 | −0.0176883193 | −0.0786362064 | −0.0609478871 |
| 12 | −0.0194881626 | −0.0835634805 | −0.0640753179 |
| 14 | −0.0209908578 | −0.0872753290 | −0.0662844712 |
| 16 | −0.0222708990 | −0.0902037775 | −0.0679328785 |
| 18 | −0.0233830732 | −0.0925954634 | −0.0692123901 |
| 20 | −0.0243655725 | −0.0946007679 | −0.0702351955 |
| 22 | −0.0252452627 | −0.0963170183 | −0.0710717556 |
| 24 | −0.0260415528 | −0.0978103244 | −0.0717687716 |
| 26 | −0.0267688671 | −0.0991273624 | −0.0723584952 |
| 28 | −0.0274382013 | −0.1003021397 | −0.0728639383 |
| 30 | −0.0280581232 | −0.1013600906 | −0.0733019674 |
| 32 | −0.0286354356 | −0.1023206640 | −0.0736852285 |
| 34 | −0.0291756284 | −0.1031990186 | −0.0740233902 |
| 36 | −0.0296831955 | −0.1040071669 | −0.0743239714 |
| 38 | −0.0301618611 | −0.1047547685 | −0.0745929075 |
| 40 | −0.0306147460 | −0.1054496923 | −0.0748349463 |
| 42 | −0.0310444913 | −0.1060984224 | −0.0750539311 |
| 44 | −0.0314533516 | −0.1067063577 | −0.0752530061 |
| 46 | −0.0318432669 | −0.1072780356 | −0.0754347687 |
| 48 | −0.0322159188 | −0.1078173020 | −0.0756013832 |

TABLE III. The value of $A_1$ for $L_s = 6$, 8, 10, 12, 16 and $0.7 \leq am_5 \leq 1.3$.

| | $am_5$ | | | | | | |
|---|---|---|---|---|---|---|---|
| $L_s$ | 0.7 | 0.8 | 0.9 | 1.0 | 1.1 | 1.2 | 1.3 |
| 6 | ... | ... | 0.0102(8) | 0.0125(9) | 0.0145(7) | ... | ... |
| 8 | ... | 0.0047(4) | 0.0074(9) | 0.0097(9) | 0.0119(9) | 0.0135(4) | ... |
| 10 | 0.0004(2) | 0.0040(9) | 0.0066(9) | 0.0090(9) | 0.0111(9) | 0.0129(9) | 0.0135(2) |
| 12 | 0.0007(9) | 0.0037(9) | 0.0064(9) | 0.0088(9) | 0.0108(9) | 0.0126(9) | 0.0139(8) |
| 16 | 0.0006(10) | 0.0036(9) | 0.0063(9) | 0.0087(9) | 0.0107(9) | 0.0125(9) | 0.0137(10) |

TABLE IV. The relative deviation $\delta^{(0)}_{1,1}$ with $am_5 = 1$ and $\theta = \pi/5$ for tree-level boundary $O(a)$ improvement.

| | $L_s$ | | | | |
|---|---|---|---|---|---|
| $L/a$ | 6 | 8 | 10 | 12 | 16 |
| 4 | −0.000602 | −0.000518 | −0.000527 | −0.000538 | −0.000545 |
| 6 | −0.000753 | −0.000562 | −0.000522 | −0.000516 | −0.000517 |
| 8 | −0.000908 | −0.000737 | −0.000688 | −0.000674 | −0.000669 |
| 10 | −0.000825 | −0.000695 | −0.000655 | −0.000643 | −0.000637 |
| 12 | −0.000701 | −0.000599 | −0.000569 | −0.000560 | −0.000555 |
| 14 | −0.000595 | −0.000511 | −0.000487 | −0.000480 | −0.000476 |
| 16 | −0.000512 | −0.000439 | −0.000419 | −0.000413 | −0.000411 |
| 18 | −0.000448 | −0.000383 | −0.000365 | −0.000360 | −0.000358 |
| 20 | −0.000397 | −0.000338 | −0.000322 | −0.000318 | −0.000316 |
| 22 | −0.000356 | −0.000302 | −0.000288 | −0.000284 | −0.000282 |
| 24 | −0.000322 | −0.000273 | −0.000259 | −0.000256 | −0.000254 |

TABLE V. The relative deviation $\delta^{(1)}_{1,1}$ with $am_5 = 1$ and $\theta = \pi/5$ for one-loop-level boundary $O(a)$ improvement.

| | $L_s$ | | | | |
|---|---|---|---|---|---|
| $L/a$ | 6 | 8 | 10 | 12 | 16 |
| 4 | 0.000955 | 0.000701 | 0.000597 | 0.000558 | 0.000539 |
| 6 | 0.000286 | 0.000251 | 0.000227 | 0.000214 | 0.000206 |
| 8 | −0.000129 | −0.000128 | −0.000126 | −0.000127 | −0.000127 |
| 10 | −0.000202 | −0.000207 | −0.000206 | −0.000204 | −0.000203 |
| 12 | −0.000182 | −0.000193 | −0.000195 | −0.000194 | −0.000194 |
| 14 | −0.000150 | −0.000162 | −0.000166 | −0.000166 | −0.000166 |
| 16 | −0.000123 | −0.000134 | −0.000138 | −0.000139 | −0.000140 |
| 18 | −0.000101 | −0.000112 | −0.000115 | −0.000117 | −0.000117 |
| 20 | −0.000085 | −0.000094 | −0.000098 | −0.000099 | −0.000099 |
| 22 | −0.000072 | −0.000080 | −0.000083 | −0.000084 | −0.000085 |
| 24 | −0.000062 | −0.000069 | −0.000072 | −0.000073 | −0.000074 |


[1] D. B. Kaplan, Phys. Lett. B **288**, 342 (1992).
[2] Y. Shamir, Nucl. Phys. **B406**, 90 (1993).
[3] H. Neuberger, Phys. Lett. B **417**, 141 (1998).
[4] J. Noaki *et al.*, arXiv:0810.1360.
[5] C. Allton *et al.* (RBC-UKQCD Collaboration), Phys. Rev. D **78**, 114509 (2008).
[6] Y. Aoki *et al.*, Phys. Rev. D **78**, 054510 (2008).
[7] C. Sturm, Y. Aoki, N. Christ, T. Izubuchi, C. Sachrajda, and A. Soni, Phys. Rev. D **80**, 014501 (2009).
[8] M. Lüscher, R. Narayanan, P. Weisz, and U. Wolff, Nucl. Phys. **B384**, 168 (1992).
[9] Y. Taniguchi, J. High Energy Phys. 12 (2005) 037.
[10] Y. Taniguchi, J. High Energy Phys. 10 (2006) 027.
[11] Y. Nakamura, S. Aoki, Y. Taniguchi, and T. Yoshie (CP-PACS Collaboration), Phys. Rev. D **78**, 034502 (2008).
[12] S. Sint, arXiv:1008.4857.
[13] M. Lüscher, J. High Energy Phys. 05 (2006) 042.
[14] S. Takeda, Nucl. Phys. **B796**, 402 (2008).
[15] S. Sint, Nucl. Phys. **B421**, 135 (1994).
[16] N. H. Christ and G. Liu, Nucl. Phys. B, Proc. Suppl. **129–130**, 272 (2004).
[17] Y. Kikukawa and T. Noguchi, arXiv:hep-lat/9902022.
[18] Y. Kikukawa, Nucl. Phys. **B584**, 511 (2000).
[19] S. Sint and R. Sommer, Nucl. Phys. **B465**, 71 (1996).
[20] M. Lüscher, R. Sommer, P. Weisz, and U. Wolff, Nucl. Phys. **B413**, 481 (1994).
[21] A. Bode, P. Weisz, and U. Wolff (ALPHA Collaboration), Nucl. Phys. **B576**, 517 (2000); **B600**, 453(E) (2001).
[22] S. Aoki and Y. Kuramashi, Phys. Rev. D **68**, 034507 (2003).
[23] M. Lüscher, P. Weisz, and U. Wolff, Nucl. Phys. **B359**, 221 (1991).